

# Constraining CMB-consistent primordial voids with cluster evolution

H. M. Athi<sup>1</sup>?, J. Silk<sup>1</sup>, L. M. G. Riths<sup>2</sup> and M. Kunz<sup>3</sup>

<sup>1</sup>Astrophysics, University of Oxford, Denys Wilkinson Building, Keble Road, Oxford OX1 3RH, UK

<sup>2</sup>Astrophysics, UNSW, Sydney, NSW 2052, Australia

<sup>3</sup>Astronomy Centre, University of Sussex, Brighton BN1 9QH, UK

24 December 2018

## ABSTRACT

Using cosmological simulations, we make predictions for the distribution of clusters in a plausible non-gaussian model where primordial voids nucleated during inflation act together with scale-invariant adiabatic gaussian fluctuations as seeds for the formation of large-scale structure. This model agrees with most recent observations of the anisotropies of the cosmic microwave background (CMB) and can account for the excess of power measured on cluster scales by the Cosmic Background Imager (CBI), the large empty regions apparent in nearby galaxy surveys and the number of giant arcs measured in deep cluster lensing surveys. We show that the  $z = 0$  cluster mass function differs from predictions for a standard CDM cosmology with the same  $\Omega_m$ . Moreover, as massive clusters also form much earlier in the "void" scenario, we show that integrated number counts of SZ sources and simple statistics of strong lensing can easily falsify this model.

**Key words:** cosmology: theory { large-scale structure of the Universe { cosmic microwave background galaxies: clusters: general

## 1 INTRODUCTION

The emergence of the CDM scenario as the standard model for both the evolution of the cosmological background and the development of large-scale structure has recently received dramatic confirmation from the WMAP microwave background experiment (Spergel et al. 2003). In this picture of minimal complexity, adiabatic gaussian fluctuations in the energy density with scale-invariant power law power spectrum generated in the early Universe are stretched during inflation to astrophysically relevant scales. Gravitational instability is then responsible for amplifying the resulting overdensities and for the collapse of structure. In hierarchical models like cold dark matter (CDM), small objects collapse first and the more massive clusters form relatively recently. Although successful in many aspects, the ability of the model to reproduce the mass function of satellites of the Milky Way (Tully et al. 2002; Stoehr et al. 2002), the rotation curves of LSB galaxies (McGaugh et al. 2003), or the bulk properties of the stellar populations of massive ellipticals (Peebles 2001) is still uncertain, even if recent hints towards tilt and/or running of the primordial spectrum in-

dex (Peiris et al. 2003) might help resolve some of the discrepancy on small scales.

On larger scales, the voids seen in the nearby galaxy distribution (Elaad & Piran 2000; Peebles 2001; Hoyle & Vogeley 2002) or the still controversial large-scale features (Broadhurst et al. 1990; Percival et al. 2001; Frith et al. 2003) justify the development of more complex, non-gaussian scenarios where linear, two-point predictions are in agreement with observations of the CMB, with the hope that simulations of galaxy formation in different environments and of the Lyman-forest will agree with observations at least at the level of CDM (Kaumann et al. 1999; Springel et al. 2001; Athi<sup>1</sup> & White 2002; Croft et al. 2002, see also van den Bosch et al. 2003).

We consider one such alternative to the concordance model, where primordial bubbles of true vacuum that formed in a first-order phase transition during inflation can survive to the present day and result in cosmological voids (La 1991; Liddle & Wands 1991; Ochionero et al. 1997; Ochionero & Amendola 1994). This model is typically implemented in the context of so-called 'extended inflation' (La & Steinhardt 1989). With reasonable values for the distribution of voids, G ri ths et al. (2003, hereafter G03) (see also Baccigalupi et al. 1997; Baccigalupi & Perrotta 2000) have

? Email: hxm@astro.ox.ac.uk

shown the angular power spectrum of CMB temperature anisotropies in this primordial void model with CDM-type cosmological parameters to fit the observations at  $1 < 800$ . The signature of voids emerges at  $1 > 1000$  and can account for the excess power seen by the Cosmic Background Imager (CBI) on cluster scales ( $l < 2500$ ) if it is not due to an underestimation of the Sunyaev-Zel'dovich (SZ) effect. While viable in terms of the temperature angular power spectrum, we note that Corasaniti et al. (2001) derive constraints on the underdensity and volume fraction of voids at recombination from the COBE-DMR three-point correlation function and that Acciagalupi & Perrotta (2000) predict non-gaussian features in the CMB temperature fluctuations that have yet to be tested against high-resolution maps.

To assess this void model from another direction, we simulate large-scale structure formation using collisionless dark matter simulations of a network of compensated voids embedded in a CDM cosmology. Due to the strong non-gaussianity, using concordance values for  $\sigma_8$ ,  $\Omega_0$  results in a present-day cluster mass function (MF) that significantly departs from the gaussian case. Non-linear structures develop much earlier in the void model, the result both of gravitational instability in the compensating dark matter shells surrounding the voids and of the large-scale motions triggered by the void + shells system. Integrating the cluster evolution up to  $z = 5$ , we show that simple number counts of SZ sources and optical depth to strong lensing are significantly enhanced with respect to the CDM scenario and that such observations may easily rule out the void model. Note that Amendola & Borgani (1994) have compared the angular two-point correlation function and the scaling of higher-order moments of a series of models with primordial voids to available observations of galaxy clustering. Their approach was however semi-analytical and lacked dynamical evolution of the structures.

This paper is organised as follows. In Section 2, we recall the parameters of the void distribution and the approximations we make, the same as G03. In Section 3, we discuss the set-up of the initial conditions, make simple checks and present results at  $z = 0$ . We deal with the high- $z$  cluster evolution in Section 4, and motivate our choice of observables. We conclude in Section 5.

## 2 PHENOMENOLOGICAL MODEL

### 2.1 Parameters

We take the parameters of the fiducial void model of G03. The background is a flat, dark energy dominated cosmology with  $h = 0.7$ ,  $\Omega_0 = 0.3$ ,  $\Omega_b = 0.7$ . We assume that fluctuations of the field driving inflation produce the usual gaussian adiabatic scale invariant perturbations, iterated as they reenter the horizon by a CDM transfer function. Variants of extended inflation predict that the first bubbles to nucleate during the phase transition can reach cosmological sizes at recombination. The cumulative number density of the voids is taken to be :

$$N_V(r) = A r \quad (1)$$

where  $r$  is the physical void radius,  $A$  a normalisation constant adjusted to match the present-day void filling fraction of

voids seen in galaxy redshift surveys, and the exponent is related to the gravitational coupling  $\lambda$  of the inflation if extended inflation can be described with a Brans-Dicke formulation :

$$\lambda = 3 + \frac{4}{1 + 1/2} \quad (2)$$

Solar system experiments require  $\lambda > 3500$  (Will 2001) and we will take here  $\lambda = 3$ . The cut-off at small radius is also chosen to agree with redshift surveys. Pionis & Basilakos (2002); Hoyle & Vogeley (2002) measured the typical size of voids in the PSCz and UZC surveys and found that up to half of the volume of the universe is underdense with  $\delta_{\text{gal}} = \delta_{\text{gal}} < -0.9$ . The void radii they obtain range from  $10$  to  $30 h^{-1} \text{ Mpc}$  with an average of  $15 h^{-1} \text{ Mpc}$ . We take accordingly  $r_{\text{min}} = 10 h^{-1} \text{ Mpc}$ . Furthermore, G03 constrain the maximum radius of the voids to  $r_{\text{max}} = 25 h^{-1} \text{ Mpc}$  to remain consistent with the observed CMB angular power spectrum at  $2000 < l < 3000$ . Physical assumptions for the cut-offs are that (1) on sub-horizon scales, matter flows relativistically back into the voids after inflation, and erases the small voids with radius  $r < 10 h^{-1} \text{ Mpc}$  (Ochionero et al. 1997) and that (2) the tunneling probability of inflationary bubbles is modulated through the coupling to another field, resulting in a maximum radius. Last, we take an observed  $z = 0$  void filling fraction of  $f_{\text{voids}} = 40\%$ .

### 2.2 Approximations

In this paragraph, we briefly recall the assumed profile and spatial distribution of the voids.

We neglect the contribution of baryons as our purpose is to obtain statistics for massive clusters, where the dynamics is led by the dark matter. As the CDM becomes non-relativistic early in the expansion, it travels only minimally into the voids which reenter the horizon later and are of interest for structure formation. On the other hand, due to the tight coupling to photons, baryons will fill voids which are within the horizon before decoupling at the adiabatic sound speed (Liddle & Wands 1991), before gravitation takes over radiation pressure. If at some point the mass of baryons inside the voids reaches a substantial fraction of the mass of the shell, the growth of the void radius will be slower than expected for a fully empty, compensated region. We simply mention that the precise dynamics of void filling by the baryons is complex and needs further study when comparing for instance the high-redshift distribution of voids with the clustering of the Lyman-alpha forest, and that the precise density profile of the voids depends on the physics of reheating and of the subsequent filling by baryons.

Smooth void density profiles have been considered for analytical work : rounded step functions (Hoffman et al. 1983; Martel & Wasserman 1990), exponentials (Hausman et al. 1983) or periodic functions (Acciagalupi 1998). However, with the exception of Regos & Geller (1991) who also use a smooth initial profile, numerical simulations of void evolution using particles often approximate voids as "top-hat" underdensities (White & Ostriker 1990; Robinson & Baker 2000, hereafter WO, R00). These authors do not consider any particular physical model, but rather use generic templates of single voids or void networks. Here, to follow

G 03 we suppose that the voids at decoupling are spherical "top-hat" underdensities with  $\delta_M = \delta_m = -1$  surrounded by a thin compensating shell of dark matter.

In an EdS cosmology, the shell density profile can be exactly derived from the self-similar solution of the evolution of a spherical underdensity (Bertschinger 1985, hereafter B 85). We assume that all the matter is swept up during the expansion of the void ends in the compensating shell around it. This behaviour results naturally from the expansion of an underdense region in an EdS cosmology (where the thickness of the shell is very slowly growing, see B 85), a very good approximation to CDM when we start the simulations. Recall that G 03 assume for simplicity an EdS cosmology to compute the void contribution to the angular power spectrum of the CM B anisotropies, and add the result to the power spectrum of the concordance CDM model. This makes sense, because (1) most of this contribution comes from voids close to the last scattering surface (LSS) where CDM is similar to EdS and (2) the contribution to the power spectrum varies smoothly with  $l$ , reducing the impact of the correction for angular diameter distance.

As G 03 we ensure that the voids do not initially overlap, although there seems to be no physical motivation for such a restriction. In practice, given the starting redshift we choose, our results depend very weakly on this hypothesis. Finally, the positions of centers of the voids are initially uncorrelated.

### 3 SIMULATING THE VOID NETWORK

#### 3.1 Initial conditions

We focus on two collisionless simulations of side  $200 h^{-1} \text{ Mpc}$  using  $64^3$  particles, carried out with the publicly available hydra N-body, hydrodynamics code in its AP<sup>3</sup>M version<sup>Y</sup>. The first simulation, called G, is a gaussian CDM model with concordance parameters, the second, V, is the CDM + voids non-gaussian fiducial model of G 03. Except for the total initial displacement field, all simulation parameters are similar in the two cases. The simulations employ fixed comoving Plummer softening of  $0.1 h^{-1} \text{ Mpc}$ .

The size of the box is a compromise between the necessity of having enough primordial voids covering the whole radius range at  $z = 0$ ,  $[10:25] h^{-1} \text{ Mpc}$ , and the mass resolution. (The comoving radius range is  $[3:76] h^{-1} \text{ Mpc}$  at the starting redshift  $z_{\text{init}}$ .) Even independently of the halo resolving power,  $N_{\text{parts}} = 64^3$  is a stringent lower limit to the number of particles as simulations need to (1) propagate information about the smallest voids present at the starting redshift and (2) have sufficient initial power in the cosmological displacement field with respect to the power due to shot noise at the Nyquist frequency of the particles not to alter the formation of the smallest haloes one can resolve. While condition (1) is easy to verify, we will use G to check (2) with the MF of dark matter haloes at  $z = 0$ . We find haloes with a friends-of-friends algorithm (Davidsen et al. 1985) with linking length 0.2 times the mean interparticle

separation, and keep only the groups with more than 10 particles. The minimum total halo mass we can then resolve is  $M_{\text{min}} = 2.53 \times 10^{13} h^{-1} \text{ M}_\odot$ .

We start from a glass distribution of particles (Baugh et al. 1995; White 1996). In G, the initial displacement field is given by the usual Zel'dovich approximation applied to the CDM power spectrum, normalized to a present  $z = 0:9$ . We compute it on a  $128^3$  mesh. In V, it is the same field for particles outside any primordial void and the displacement predicted by the similarity solution of B 85 taken in the EdS regime ( $r / t^{4/5}$  where  $r$  is the physical void radius and  $t$  the time) for all particles that fall within a primordial void. Given the assumptions of paragraph 2.2, we put all particles falling in a void at its radius, and assign them the radial velocity of the expanding shell, following W 0. In that sense, our V simulation would be close to that of a "spontaneous creation" of voids at  $z_{\text{init}}$ .

To follow G 03, we use the similarity solution of an EdS universe (using the EdS time elapsed from  $z_{\text{init}}$  to  $z = 0$ ) to compute the initial radii and shell velocities of the voids, although we run the simulations with a CDM background. In doing so, we neglect differences expected with respect to EdS in the initial radii if voids were scaled back from  $z = 0$  using a theoretical solution for a CDM cosmology. However, we verify below that this enables simulations to correctly reproduce single  $25 h^{-1} \text{ Mpc}$  radius voids at  $z = 0$ . Furthermore, the similarity scaling between void radius and shell velocity remains strictly valid at  $z_{\text{init}}$  as EdS is then a very good approximation to CDM (see B 85).

The starting redshift for particle simulations of cosmological models with gaussian initial conditions is usually set by requiring the maximum particle displacement to be a few percents of the mean interparticle distance. An upper limit on  $z_{\text{init}}$  results from condition (1) on  $N_{\text{parts}}$  and translates the lower limit on the amplitude of the power spectrum of the initial perturbations. To choose  $z_{\text{init}}$  for the collisionless cosmological simulations of a non-gaussian model with primordial voids, R 00 ensure that  $\sigma^2 < 0:15$  at the Nyquist frequency of the particles and that no shell crossing occurs when initially displacing the particles. This is feasible as they compute the displacement for all their particles only from the Zel'dovich scheme applied to a linear density field. Their density field is the superposition of a gaussian field and a distribution of mildly underdense spherical regions with void  $0:1$ . Because we start our simulations with compensated empty voids, we immediately probe the non-linear regime on void scales. As a consequence, the MF of haloes that we obtain at  $z = 0$  in the void model depends on  $z_{\text{init}}$ . Therefore we start the simulations soon after decoupling with  $z_{\text{init}} = 1000$  noting that our results will underestimate the abundance of the haloes we find at low redshift, but this is enough for the points we want to make. Independently of the shape of the one-point PDF of the initial overdensity field, a worry from such a high starting redshift is that numerical integration of the equations of motion might suppress the growth of small-scale modes (see the introduction of Scoccimarro 1998). Again, we use below the  $z = 0$  halo MF of G to check that this does not affect our conclusions.

<sup>Y</sup> <http://hydra.mcmaster.ca/hydra/index.html>

### 3.2 Consistency checks

To check the accuracy of the particle-mesh scheme and the effect of periodic boundary conditions, we simulate with `hydra` the growth from  $z_{\text{init}}$  of a single void with final radius  $25 \text{ h}^{-1} \text{ Mpc}$  centered on a  $100 \text{ h}^{-1} \text{ Mpc}$  box without the gaussian part of the displacement field, in a EdS universe. We use the EdS similarity solution to scale back to  $z_{\text{init}}$ . At  $z = 0$ , we find that the total mass enclosed inside 99% (98%) of the inner shell radius of  $25 \text{ h}^{-1} \text{ Mpc}$  is 9% (3%) of that expected in a similar volume with mean density. The same test is repeated with the scaling method described above for simulations in a CDM background and we find a ‘leaking’ mass fraction of 3% (0%). We check that in both cases this remaining mass is mostly contributed by particles of clusters formed on the shell and that the particle distribution is smooth beyond a  $25 \text{ h}^{-1} \text{ Mpc}$  radius.

We verify that the  $z = 0$  halo MF of the G simulation gives results in agreement with the fitting formula of Jenkins et al. (2001, hereafter J01) and that it is robust against changes in  $z_{\text{init}}$ . (Using  $N_{\text{parts}} = 32^3$  for the G simulation results in an excess of low mass haloes if  $z_{\text{init}} = 1000$ ). As expected, in the CDM + voids model, for a given  $z = 0$  mass threshold  $M_{\text{th}}$ , the cumulative number of haloes more massive than  $M_{\text{th}}$  is an increasing function of  $z_{\text{init}}$ . During both simulations, the ratio of the change in the Layzer-Irvine energy integral to the potential energy is always less than 3%. Also, the validity of the Zeldovich approximation on large scales when setting up the initial conditions is checked by the growth of the largest modes of the simulation, in agreement with linear theory down to  $z = 0$ . Last, we perform two other simulations of the void model, changing both the gaussian random perturbation field and the positions of the voids, and find results very similar to those for V.

### 3.3 Results at $z = 0$

The Fig. 1 shows the projected 3D density of two slices of side  $200 \text{ h}^{-1} \text{ Mpc}$  and thickness  $20 \text{ h}^{-1} \text{ Mpc}$  cut at the same position through the G and V simulations (left and right panels respectively). Recall that the two simulations use the same initial gaussian displacement field, which in the case V is combined with the displacement due to the primordial voids. The color scale is the same in the two cases. The larger number of dark matter clumps is obvious in V; together with a very clear ‘honeycomb’ structure, a result from the expansion of the voids.

Fig. 2 gives the initial and  $z = 0$  real-space overdensity power spectra (dashed and solid lines for the G and V simulations respectively). To guide the eye, diamonds show the galaxy power spectrum (in redshift space) of the PSCz redshift survey (Sutherland et al. 1999). The imprint of voids is already significant at  $z_{\text{init}}$ . At  $z = 0$ , non-linear power is larger than for the CDM model, and extends to larger scales. Of course a precise comparison between the V power spectrum and the data is not possible at this point, as one needs to correct for redshift-space distortions and bias, two quantities that might be significantly different in the CDM + voids model with respect to CDM, and fall beyond the scope of this work.

The main panel of Fig. 3 compares the halo MF measured at  $z = 2.1$  and 0 from left to right in the G and V

simulations (dashed and solid lines respectively) to the fitting formula of J01 (dash-dotted lines). While the G simulation agrees well with J01, there are significantly more haloes in the V simulation at  $z = 0$ . We find respectively 2 and 6 haloes with  $M_{\text{tot}} > 10^{15} \text{ h}^{-1} \text{ M}_{\odot}$  in the G and V simulation. (Recall that the gaussian part of the initial overdensity field is normalized to the same present-day  $\delta = 0.9$ .) The insert in Fig. 3 gives the differential halo MF measured around  $10^{14} \text{ h}^{-1} \text{ M}_{\odot}$ . The excess of the non-gaussian model is apparent at all mass scales greater than  $5 \times 10^{13} \text{ h}^{-1} \text{ M}_{\odot}$ .

Bahcall & Cen (1993) give  $N_{>M} = 2.1 \times 10^6 \text{ h}^3 \text{ Mpc}^3$  at  $M = 4 \times 10^{14} \text{ h}^{-1} \text{ M}_{\odot}$ , shown by the triangle in Fig. 3, assuming their uncertainty factor of 1.3 in the mass of rich clusters, shown with the horizontal error bar. Using more recent data, Bahcall & Bode (2003) derive conservative limits for the abundance of clusters with  $M_{\text{tot}} > 8 \times 10^{14} \text{ h}^{-1} \text{ M}_{\odot}$ . These are shown by the diamond and square in Fig. 3 for  $z = 0.05$  and the period  $z = 0.65$  to 0.9 respectively with their 68% per cent confidence interval. Here, the vertical error bar also accounts for the uncertainty in the mass threshold. The present-day MF of the V simulation is therefore only marginally consistent with the data, all the more as we underestimate the abundance of its haloes at  $z = 0$ . In fact, the difference of the fiducial model of G03 with respect to CDM is much more obvious in the intermediate and high-mass functions. In the following we will consequently use integrated cluster counts as a stronger signature of the void model.

## 4 DERIVATIVE OBSERVATIONAL CONSTRAINTS

In this Section, we make predictions for the thermal SZ effect and for simple statistics of strong lensing. We show that they differ substantially in the primordial voids model from the values for a CDM cosmology that it is not necessary to consider more complex observables like the cosmic shear or the clustering of the Lyman-forest which could also bring out the presence of primordial voids.

### 4.1 SZ source counts

We first estimate the counts expected from the detection of the cluster thermal SZ effect, up to  $z = 5$ . Kay et al. (2001) make detailed analytical predictions for the SZ number counts expected for the Planck satellite using large numerical simulations of cluster formation in gaussian CDM cosmologies. We follow the same approach but with simplifying assumptions. We use 30 simulation outputs for G and V from  $z = 0$  to  $z = 5$ . Each dump has a comoving size  $200 \text{ h}^{-1} \text{ Mpc}$  and we find their DM haloes above the minimum mass threshold  $M_{\text{min}}$ . For simplicity we assume for each halo an isothermal profile for the gas (see, e.g., Barbosa et al. 1996) with total mass  $M_{\text{gas}} = f_b M_{\text{tot}}$  where  $f_b = 0.13$  is the cosmic baryon fraction. Taking the clusters to be point sources, we compute the magnitude of the flux change observed against the CMB at the Planck satellite frequencies 143 and 353 GHz, on both sides of the zero-point of the SZ thermal effect (217 GHz). Fig. 4 shows the minimum SZ flux that the simulations can resolve as a function of  $z$ . In the following, we show results for fluxes  $S > 20 \text{ mJy}$ . As this

Figure 1. Left and right panels : projected 3D density in slices cut at the same position through the gaussian ( CDM ) and CDM + voids simulations respectively. The side and thickness are 200 and  $20 h^{-1} Mpc$ . The gaussian initial displacement field is the same in both simulations. The color scale is the same for the two panels. Note the larger number of haloes in the void model and its clear "honeycomb" structure.

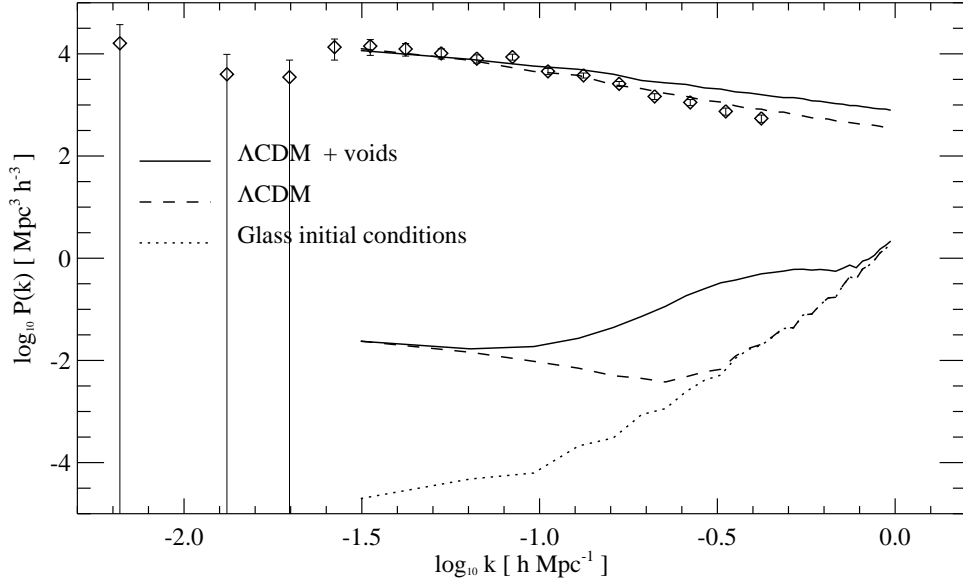


Figure 2. Real-space overdensity power spectrum at  $z = 1000$  and  $z = 0$  of the gaussian ( CDM ) and non-gaussian ( CDM + voids ) simulations : dashed and solid lines respectively. The diamonds give the redshift-space power spectrum of PSCz galaxies (Sutherland et al. 1999). The dotted line is the power spectrum of the raw glass file, for comparison. Note the signature of the voids in the initial conditions and the stronger  $z = 0$  non-linear power in the void model.

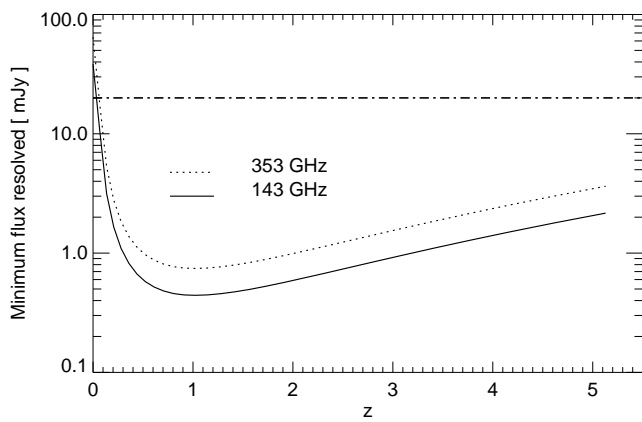


Figure 4. 143 and 353 GHz resolution limit for the cluster thermal SZ effect in the simulations as a function of redshift. We restrict the analysis to sources brighter than 20 mJy (dash-dotted line).

is below the simulation resolution for the first box (spanning  $z = 0$  to 0.07), we prefer not to extrapolate the mass function, and more conservatively start integrating outwards from  $200 h^{-1} Mpc$  away.

Fig. 5 gives the expected redshift distribution of SZ sources with  $S > 20 mJy$  in the CDM + voids and CDM

models (solid and dotted, dashed and dash-dotted lines respectively), for 143 and 353 GHz. The curves have been fitted by 3rd-order polynomials in the relevant range. While there are no sources with  $S_{143, 353 \text{ GHz}} > 20 \text{ mJy}$  at  $z > 1.6$  ( $z > 2.2$ ) in G, the distribution of such objects in the void model extends up to  $z = 5$  and is also much steeper. This is easily seen in Fig. 6, where we plot the cumulative contribution of the sources as a function of redshift. A round  $z = 1$  for example in Fig. 5, the overall effect of the primordial non-gaussianity is a strong enhancement by a factor of  $> 7 (8)$  of the counts per redshift at 143 (353) GHz. The gain is much higher at  $z = 1.5$ . In reality, there will be a number of sources with  $S_{143, 353 \text{ GHz}} > 20 \text{ mJy}$  at  $z > 5$  in the void model, as the results shown here provide only a lower limit to the counts, but the difference with respect to CDM is already very significant and SZ surveys may easily falsify the void model. To see how this conclusion varies with sensitivity, Fig. 7 gives the number counts of SZ sources expected (up to  $z = 5$ ) in the CDM (dashed and dash-dotted lines) and CDM + voids (solid and dotted lines) models as a function of the flux threshold. Above a flux limit of 20 mJy, there are  $\sim 10 (20)$  times more integrated counts at 143 (353) GHz in the CDM + voids model compared to CDM. The sensitivity of Planck to the SZ effect is of order 30 mJy (Bartelmann 2001; Kay et al. 2001), and the corresponding counts are enhanced by an order of magnitude at the two frequencies. Even when con-

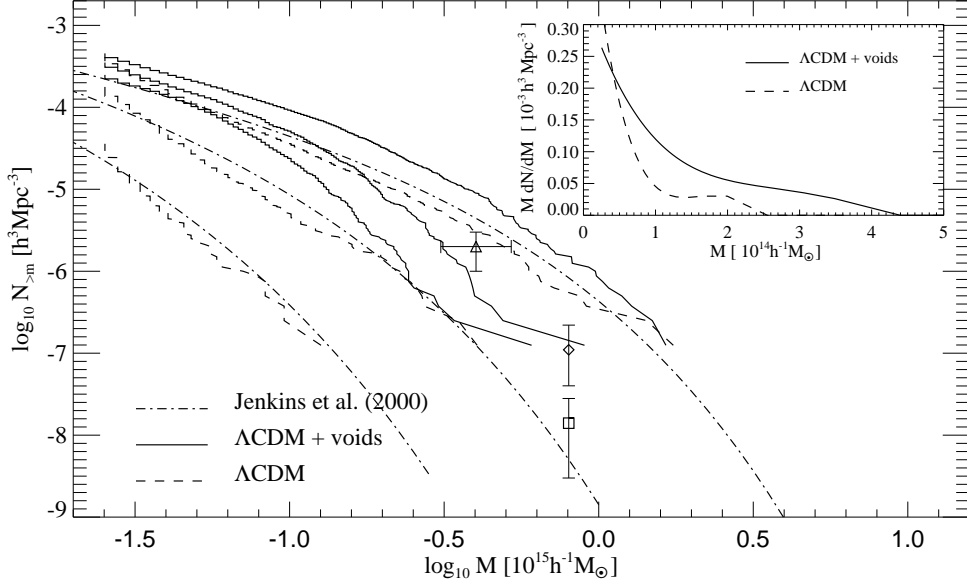


Figure 3. Main panel : mass functions of the gaussian ( CDM ) and non-gaussian ( CDM + voids) simulations : dashed and solid lines respectively, measured at  $z = 2, 1$  and  $0$  from left to right. The dash-dotted line is the fitting formula of J01 to CDM. The triangle gives the normalisation at  $4 \times 10^4 h^{-1} M_\odot$  of the cluster mass function of Bahcall & Cen (1993), the horizontal and vertical error bars show uncertainties of a factor 1.3 in the mass of rich clusters and  $1 \times 10^{-6} h^3 M_\odot \text{pc}^{-3}$  in their abundance. The diamond and square show the abundances deduced by Bahcall & Bode (2003) above a conservative limit of  $8 \times 10^{14} h^{-1} M_\odot$  for  $z = 0.05$  and the period  $z = 0.65$  to  $0.9$  respectively. The vertical error bars show their 68% confidence interval and accounts for the uncertainty in the mass threshold. Insert : differential mass functions  $dN = d \ln M$  of the gaussian ( CDM ) and non-gaussian ( CDM + voids) simulations : dashed and solid lines respectively, measured at  $z = 0$  up to  $5 \times 10^{14} h^{-1} M_\odot$ .

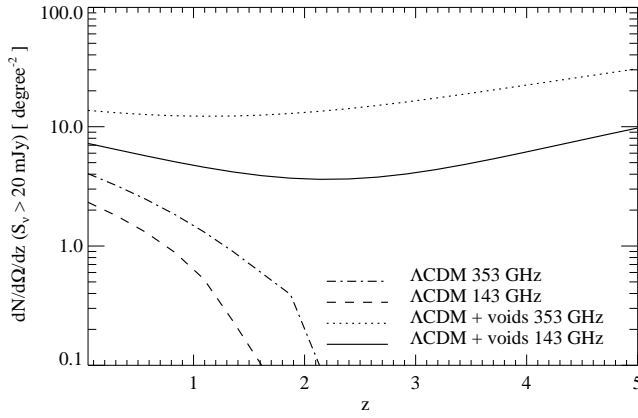


Figure 5. Redshift distribution of the sources with flux  $S_{143,353 \text{ GHz}} > 20 \text{ mJy}$  in the CDM (dashed and dash-dotted lines) and CDM + voids (solid and dotted lines) simulations.

sidering only sources brighter than 100 mJy, the factor of 3 between the models may be sufficient to rule out primordial voids, even if a more detailed computation is needed at this level of difference. Among many ground-based examples, the Bonn-Berkeley APEX - SZ survey<sup>z</sup> will cover 100

<sup>z</sup> <http://bolo.berkeley.edu/apexsz/>

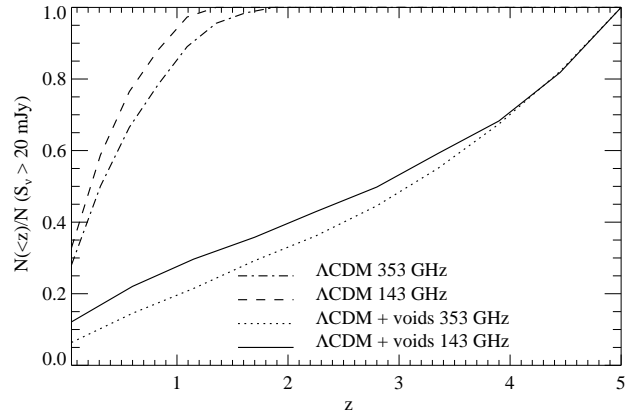


Figure 6. Cumulative version of Fig. 5.

square degrees and is expected to reach a sensitivity of 3 mJy at 150 GHz. This 300-hour experiment will detect 1000 clusters with mass  $M_{\text{tot}} > 2 \times 10^{14} h^{-1} M_\odot$  up to  $z = 2$  (assuming a CDM model) and provide strong constraints on non-gaussian models like primordial voids.

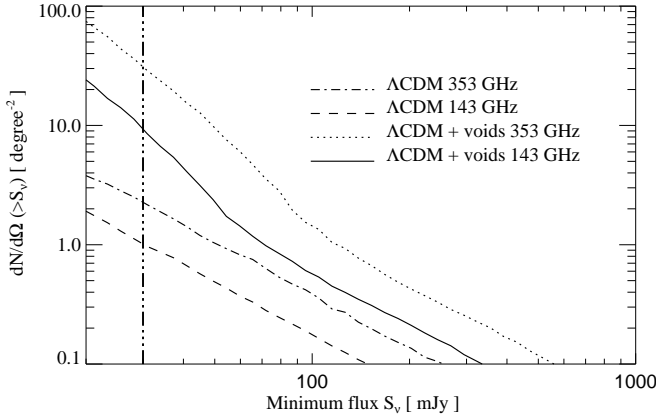


Figure 7. Number counts of SZ sources to  $z = 5$  in the CDM (dashed and dash-dotted lines) and CDM + voids (solid and dotted lines) models as a function of the minimum flux  $S_{\min}$  at 143 and 353 GHz. Note the strong enhancement (factor 20) of the counts above  $S_{\min} = 20$  mJy at 353 GHz in the model with primordial voids. The vertical line shows the sensitivity of Planck; at this level, number counts differ by a factor 10.

#### 4.2 Strong lensing

The statistics of strong amplification of images of background sources by massive concentrated structures is a powerful probe of the cosmological parameters (for example, Bartelmann et al. 1998). Of course, they will also be directly affected by the kind of primordial non-gaussianity considered here.

We assume that only the clusters that we can resolve in the simulations, ( $M_{\text{tot}} - M_{\min}$ ) produce strong lenses. We model the haloes with singular isothermal spheres (SIS) (Peacock 1982) and measure their velocity dispersions directly from the simulations. Perrotta et al. (2002) derive analytical predictions with NFW profiles for the differential amplification probability  $P(A)$  and compare them to the predictions obtained with SIS profiles. For sources at  $z = 4$  and 7, at  $A < 3$  they find their CDM model with NFW profiles to be more efficient than with SIS profiles. At  $A > 7$ , SIS profiles yield the higher  $P(A)$ , but the probabilities for NFW and SIS profiles stay within a factor 3 of each other even at larger amplifications. We put our sources at  $z = 3$  and 5. Fig. 8 shows the cumulative probability  $P(A > A_{\min})$  that a line of sight has an amplification larger than  $A_{\min}$  in the two cosmologies and for the two values of  $z_s$ . We take the strong lensing regime to be  $A > 2$ . At  $A_{\min} > 10$ , the cumulative probability for strong lensing is a factor 10 (20) higher in the void model than in the CDM case, for  $z_s = 3$  (5). This strong enhancement justifies a posteriori the simpler SIS profile and it is our main conclusion regarding the effects of primordial voids on strong lensing. Bartelmann et al. (1998) compute the number of giant arcs expected on the whole sky for a series of gaussian CDM models and show that only open CDM models can reproduce the total number of arcs seen in the EMSS sample. In particular, their open CDM model produces an order of magnitude more giant arcs than their CDM model. This is close to the amplification of the strong lensing cross section expected in our non-gaussian CDM + voids model with

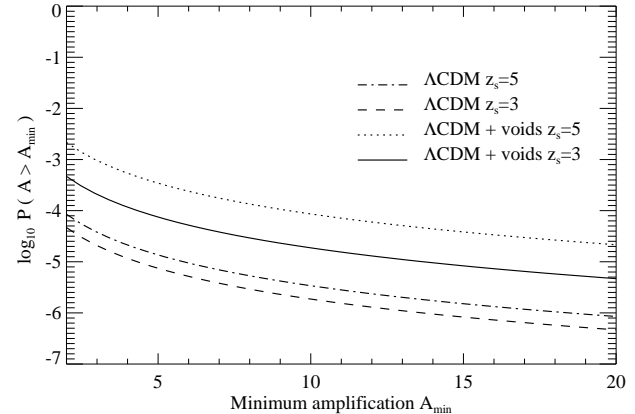


Figure 8. Probability  $P(A)$  that a line of sight is magnified by  $A > A_{\min}$  for the CDM (dashed and dash-dotted) and CDM + voids model (solid and dotted) for two source redshifts ( $z_s = 3$  and 5 respectively). We suppose that the only lenses are the massive DM haloes with  $M_{\text{tot}} > M_{\min} = 2.5 \times 10^{14} h^{-1} M_{\odot}$ , modelled as singular isothermal spheres.

respect to the concordance CDM. An early formation of massive clusters as seen in the CDM + voids model is a solution to accommodate the number counts of strong lensing distortions. However, we warn that in whatever cosmology, the impact of substructure and asphericity on the cross section for strong lensing needs better understanding (see, e.g., Meneghetti et al. 2002): recently, Gladders et al. (2003) attribute the disagreement between the counts of arcs in the Red-Sequence Cluster Survey (RCS) and theoretical expectations to the existence of a high-redshift sub-sample of the global cluster population. For this class of objects, complex internal and surrounding structure would significantly boost the cross section. We plan to tackle these issues in the future.

Fig. 9 to Fig. 11 show in turn the redshift distribution of the total optical depth  $d = dz$  to strong lensing as defined in the section 4.2 of Peacock (1999), the cumulative contribution ( $< z$ ) and the normalized redshift distribution of the optical depth  $1 = d = dz$ , for  $z_s = 3$  and 5. The total optical depth is much larger in the V than in the G simulation (note the order of magnitude ratio between the V and G curves in Fig. 9) and the peak of the redshift distribution is shifted towards higher  $z$  in V (compare the dotted and the dash-dotted curves in 10). Not only will strong distortions like giant arcs be at least an order of magnitude more common than in the usual CDM if primordial voids contribute as seeds to the formation of structure, they will also be observed up to higher redshifts given the same underlying source population.

Finally, we have assumed initially compensated voids surrounded by a thin shell growing as the underdensity expands in comoving coordinates. This large-scale configuration could per se constitute an efficient lens. In fact, Amendola et al. (1999) show that only voids with radius larger than  $100 h^{-1} M_{\odot} \text{pc}$  today induce weak gravitational lensing with a signal-to-noise ratio greater than unity in observables like color-dependent density magnification or aperture density. Even for strong underdensities like  $\text{void} = 1$ ,

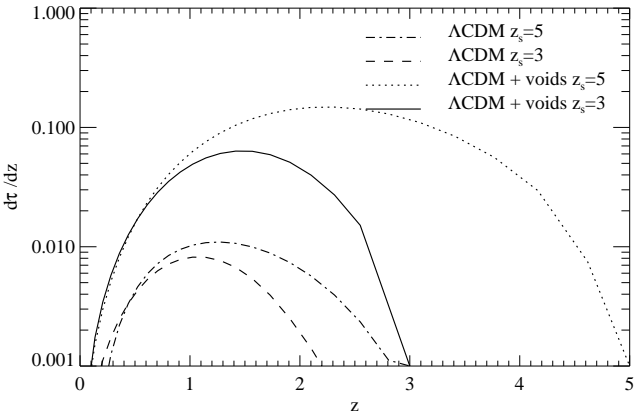


Figure 9. Redshift distribution of the optical depth to strong lensing  $d/dz$  by our resolved haloes. The legend is the same as for Fig. 8. Note the order of magnitude ratio between the primordial voids model and the gaussian CDM cosmology.

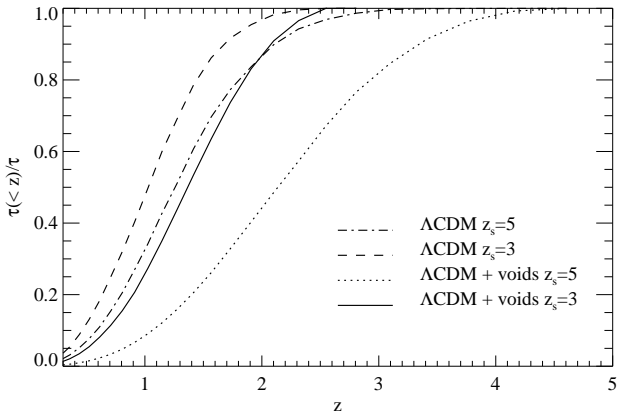


Figure 10. Same as Fig. 9 but showing the cumulative contribution to the total optical depth to strong lensing  $\langle \tau(z) \rangle$ .

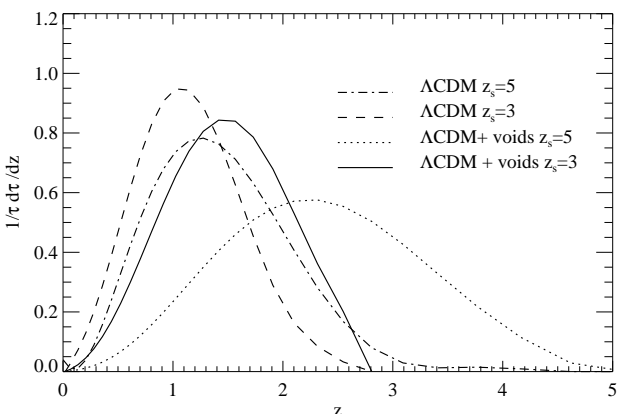


Figure 11. Same as Fig. 9 but showing the normalized redshift distribution of the optical depth to strong lensing  $1/\tau d\tau/dz$ .

none of these weak lensing techniques will be able to find a significant signature of the voids considered here.

## 5 CONCLUSIONS

We have simulated cluster formation in a physically plausible non-gaussian primordial voids model where empty and fully compensated bubbles surviving from inflation together with gaussian adiabatic CDM-type perturbations provide the seeds for the development of structure. This model shares the cosmological parameters of CDM and possesses gaussian statistics on large scales while non-gaussianity only affects the one-point distribution on cluster scales. It is an attractive alternative to CDM as it agrees with most recent measurements of the angular power spectrum of the CMB including the excess of power observed at  $l=2500$  by CBI and can explain the large voids seen in the nearby galaxy surveys (Griffiths et al. 2003). While analysis of high-resolution CMB maps using higher-order moments will provide further constraints on primordial non-gaussianity, we have shown the evolution of the cluster mass function to be a very powerful constraint at low redshift.

Due to the strong underdensities present on Mpc scales very early on compared to CDM and to the evolution of the dark matter in the compensating shell of the voids, we have found that our  $200 h^{-1} \text{Mpc-side}$ ,  $64^3$ -particle simulations which start shortly after recombination can only provide lower limits to the late-time cluster mass function of the non-gaussian model. However, the  $z=0$  mass function already shows a factor 2 to 3 more massive clusters ( $M > 10^{15} h^{-1} \text{M}_\odot$ ) in the CDM + voids model than in the concordance CDM scenario. With the expected reduction of uncertainties in the local mass function of optically selected clusters promised by the SDSS survey for example, this would already be enough to falsify primordial voids.

The evolution of the cluster mass function up to  $z=5$  in the void scenario differs strongly from that of the CDM model and seems more 'elegant' than the sole  $z=0$  mass function in distinguishing between the two. We have shown that (1) integrated number counts of SZ sources with 353 GHz flux greater than 20 mJy and (2) optical depth to strong gravitational lensing are simple but very powerful discriminants between the primordial voids model and CDM.

Both quantities are substantially enhanced in the non-gaussian case. In particular, at the sensitivity of Planck, the expected counts of SZ sources increase by an order of magnitude in the primordial voids model compared to CDM, and early cluster formation induced by the voids is able to better reproduce the number counts of giant arcs seen in the EMSS than structure formation in the concordance CDM.

Not only do such simple tests give the opportunity to rule out a particular set of models, they also more generally bring out simple constraints that have to be satisfied (e.g. with numerical simulations) as one proposes non-gaussian alternatives to the current paradigm.

## ACKNOWLEDGEMENTS

This paper has been produced using the Royal Astronomical Society/Blackwell Science L<sup>A</sup>T<sub>E</sub>X style file.

## REFERENCES

Amendola L., BORGANI S., 1994, MNRAS, 266, 191

Amendola L., Frieman J. A., Waga I., 1999, MNRAS, 309, 465

Baccigalupi C., 1998, ApJ, 496, 615

Baccigalupi C., Amendola L., Ochionero F., 1997, MNRAS, 288, 387

Baccigalupi C., Perrotta F., 2000, MNRAS, 314, 1

Bahcall N. A., Bode P., 2003, preprint, astro-ph/0212363

Bahcall N. A., Cen R., 1993, ApJ, 407, L49

Barbosa D., Bartlett J. G., Blanchard A., 1996, A&A, 314, 13

Bartelmann M., 2001, A&A, 370, 754

Bartelmann M., HUSS A., Colberg J. M., Jenkins A., Pearce F. R., 1998, A&A, 330, 1

Baugh C. M., Gaztanaga E., Efstathiou G., 1995, MNRAS, 274, 1049

Bertschinger E., 1985, ApJS, 58, 1 (B85)

Broadhurst T. J., Ellis R. S., Koo D. C., Szalay A. S., 1990, Nature, 343, 726

Corasaniti P. S., Amendola L., Ochionero F., 2001, MNRAS, 323, 677

Croft R. A. C., Hernquist L., Springel V., Westover M., White M., 2002, ApJ, 580, 634

Davis M., Efstathiou G., Frenk C. S., White S. D. M., 1985, ApJ, 292, 391

ElAd H., Piran T., 2000, MNRAS, 313, 553

Frith W. J., Busswell G. S., Fong R., Metcalfe N., Shanks T., 2003, preprint, astro-ph/0302331

G ladders M., Hoekstra H., Yee H. K. C., Hall P. B., Barrientos L. F., 2003, preprint, astro-ph/0303341

Gri ths L. M., Kunz M., Silk J., 2003, MNRAS, 339, 680 (G03)

Hausman M. A., Olson D. W., Roth B. D., 1983, ApJ, 270, 351

H oman G. L., Salpeter E. E., Wasserman I., 1983, ApJ, 263, 527

Hoyle F., Vogeley M. S., 2002, ApJ, 566, 641

Jenkins A., Frenk C. S., White S. D. M., et al., 2001, MNRAS, 321, 372 (J01)

Kau man G., Colberg J. M., Diaferio A., White S. D. M., 1999, MNRAS, 303, 188

Kay S. T., Liddle A. R., Thomas P. A., 2001, MNRAS, 325, 835

La D., 1991, PRD, 44, 1680

La D., Steinhardt P. J., 1989, PRL, 62, 376

Liddle A. R., Wanders D., 1991, MNRAS, 253, 637

Martel H., Wasserman I., 1990, ApJ, 348, 1

Mather H., White S. D. M., 2002, MNRAS, 337, 1193

McGaug S. M., Barker M. K., de Blok W. J. G., 2003, ApJ, 584, 566

Meneghetti M., Bartelmann M., Moscardini L., 2002, preprint, astro-ph/0201501

Ochionero F., Amendola L., 1994, PRD, 50, 4846

Ochionero F., Baccigalupi C., Amendola L., Monnastra S., 1997, PRD, 56, 7588

Peacock J. A., 1982, MNRAS, 199, 987

Peacock J. A., 1999, *Cosmological physics*, Cambridge University Press

Peebles P. J. E., 2001, ApJ, 557, 495

Peiris H. V., Komatsu E., Verde L., et al., 2003, preprint, astro-ph/0302225

Percival W. J., Baugh C. M., Bland-Hawthorn J., et al., 2001, MNRAS, 327, 1297

Perrotta F., Baccigalupi C., Bartelmann M., De Zotti G., Granato G. L., 2002, MNRAS, 329, 445

P lionis M., Basilakos S., 2002, MNRAS, 330, 399

Regos E., Geller M. J., 1991, ApJ, 377, 14

Robinson J., Baker J. E., 2000, MNRAS, 311, 781 (R00)

Scoccimarro R., 1998, MNRAS, 299, 1097

Spergel D. N., Verde L., Peiris H. V., et al., 2003, preprint, astro-ph/0302209

Springel V., White S. D. M., Tormen G., Kaumann G., 2001, MNRAS, 328, 726

Stoehr F., White S. D. M., Tormen G., Springel V., 2002, MNRAS, 335, L84

Sutherland W., Tadros H., Efstathiou G., et al., 1999, MNRAS, 308, 289

Tully R. B., Somerville R., Trentham N., Verheijen M. A. W., 2002, ApJ, 569, 573

van den Bosch F. C., Mo H. J., Yang X., 2003, preprint, astro-ph/0301104

White S. D. M., 1996, in *Cosmology and Large Scale Structure, Les Houches Summer School of Theoretical Physics, Session LX*, NATO ASI

White S. D. M., Ostriker J. P., 1990, ApJ, 349, 22 (W90)

Will C. M., 2001, *Living Review of Relativity*, 4, 803

This figure "figure1.gif" is available in "gif" format from:

<http://arxiv.org/ps/astro-ph/0303519v1>